Supplementary Material for

Using step width to compare locomotor biomechanics between extinct, non-avian theropod dinosaurs and modern obligate bipeds.

P.J. Bishop*, C.J. Clemente, R.E. Weems, D.F. Graham, L.P. Lamas, J.R. Hutchinson, J. Rubenson, R.S. Wilson, S.A. Hocknull, R.S. Barrett and D.G. Lloyd.

*Corresponding author: peter.bishop@qm.qld.gov.au

Contents:

Supplementary text - detailed methods

1. Culpeper theropod trackways

1.1. Data collection

The Culpeper Crushed Stone Quarry trackways were exposed by mining operations in the quarry in the early 1990s. Upon their initial discovery, the entire set of trackways was excavated and measured by R.E.W. and colleagues [1, 2]. Unfortunately, once the trackways had been studied and measured, mining operations had to recommence, destroying them. However, a number of exemplar footprint specimens were collected and are currently housed in the Culpeper County Museum (Culpeper, Virginia), the United States Geological Survey National Center (Reston, Virginia), the Virginia Museum of Natural History (Martinsville, Virginia) and the Department of Paleobiology of the United States National Museum (Washington, D.C.).

Owing to differential preservation of footprints along the length of a given trackway, a novel technique was employed so as to facilitate a standardized measurement of pace length and bearing. Specifically, for each trackway a clear sheet of mylar film was laid on top of one of the best preserved footprints, whereupon the outline of the footprint was traced on the film with indelible pen. A small hole was then cut in the tracing at the posterior end of the impression of digit III, approximately in the centre of the footprint. By laying the traced outline on top of each footprint in the trackway and obtaining the best spatial fit between the outline and the footprint, a spot of paint was then applied to the footprints through the hole in the film. Thus, even if a given footprint was not completely preserved, an approximately 'homologous' landmark could be identified and marked (figure 1b of main text). Pace lengths and bearings were then measured using the paint spots as the points of reference (figure 1c of main text). Pace length was measured using a flexible tape to the nearest inch, and pace bearings were made using a compass to the nearest degree.

All theropod footprints from the site have been previously assigned to the ichnotaxon *Kayentapus minor* [1, 2], although the taxonomic identity of the trackmakers themselves cannot be discerned with certainty. Clearly, however, they were small to medium-sized theropods [2]; the most likely candidate would be some form of basal neotheropod, similar to

Liliensternus in overall size and proportions. The similarity in morphology of all the footprints suggests that a single genus, if not species, is recorded in the trackways [1, 2].

1.2. Data analysis

From the measured pace bearings A_{N-1} and A_N, the pace angulation (in degrees) at footprint F_N was determined as

$$\theta_N = \begin{cases} 180 + (A_{N-1} - A_N) \text{ if } F_N \text{ is a left footprint} \\ 180 - (A_{N-1} - A_N) \text{ if } F_N \text{ is a right footprint} \end{cases}. \quad \text{(S1)}$$

In turn, the stride length at (opposite to) footprint F_N was calculated as

$$S_N = \sqrt{{D_{N-1}}^2 + {D_N}^2 - 2D_{N-1}D_N \cos\theta_N}\,, \quad \text{(S2)}$$

where D_{N-1} and D_N are the preceding and successive pace lengths, respectively. Step width at footprint F_N was then calculated as

$$w_N = \frac{D_N D_{N-1} \sin\theta_N}{S_N}. \quad \text{(S3)}$$

The calculated stride lengths and step widths were normalized to the estimated hip height of the trackmakers,

$$S^* = S/h, \quad \text{(S4)}$$

$$w^* = w/h, \quad \text{(S5)}$$

where h is the hip height. Hip height was estimated via the equation of Thulborn [3-5] for small to medium-sized theropods, namely,

$$h = 3.06L^{1.14}, \quad \text{(S6)}$$

where L is the mean footprint length for each trackway, as reported by Weems [2]. Normalization of stride length and step width to hip height helps to facilitate fair comparison across the separate trackways.

Of the 20 trackways measured, only eight (trackways K-4, K-5, K-10, K-11, K-14, K-15, K-17, K-20) were actually subjected to analysis. This is on account of two factors:

i. These eight trackways are the only ones that showed evidence of a marked change in speed across the preserved length of the trackway. In each of the eight trackways, relative stride length S^* significantly exceeded 1.8 across some part of their exposed length; all the other trackways show a consistent, slow walking speed (S^* generally between 1.5 and 1.8) throughout their exposed length.

ii. These trackways were all made by individuals of about the same size (estimated h of 1.10–1.2 m). By effectively controlling for body size across the individuals involved, this adds greater rigour to a comparison across trackways.

The data for the eight trackways were analysed together for two reasons. Firstly, the trackways were occasionally missing individual prints or small sets of prints throughout their length, either due to non-preservation or damage to the tracking layer. Secondly, within any single trackway, the interval over which the change in speed occurred was relatively short. For instance, in the K-15 trackway, the trackmaker accelerated from a walk ($S^* \approx 1.8$) to a fast run ($S^* \approx 3.5$) in less than five consecutive strides. Such relatively quick changes in speed afford only a limited number of data points in the transition between slow walking and running for any individual trackway. Thus, considering all the trackways together increases the size of the dataset, helping to identify any general patterns, as well as to even out individual variation.

Segments of trackways that showed 'abnormal' behaviour were excluded from analysis. Such behaviours include the trackmaker stopping, shuffling around or abruptly making a sharp turn. Also, instances where manus (hand) prints of the trackmaker were present (i.e., the trackmaker bent down to all fours, perhaps to sniff the ground) were excluded. Sections of the trackways where the trackmaker made a significant change in direction (i.e., it was making a turn) were noted. These were both included and excluded from analysis, although this had no appreciable effect on the final results. Hence, there was little, if any, confounding effect of changes in direction on the results.

2. Human kinematics

2.1. Data collection

Prior to data collection, each subject's natural walk-run transition speed was ascertained by starting them on the treadmill at a slow walking speed and gradually increasing the tread speed until they spontaneously switched to a run. This transition speed was validated by increasing the tread speed further, and then gradually decreasing the speed until the subject spontaneously switched back to a walk. For each subject, their walk-run and run-walk transition speeds were approximately the same. The use of the treadmill was chosen so as to facilitate the acquisition of a large amount of data in a short time span, and also because it was already set up and calibrated with the motion capture system; an overground racetrack of

suitable length required for this study, with calibrated cameras, was not available during the period of data collection.

So as to remove any potential confounding effects of difference in shoe designs worn by the subjects on the day of testing, they walked and ran barefoot in the experiments. For each trial, the subject initially stood still on the stationary tread, whence the tread speed was gradually increased to the desired trial speed over a period of 5–10 s. After the subject had reached a steady manner of locomotion, data recording commenced, lasting for a minimum of four strides. Subsequently, the tread speed was slowly reduced back to zero. The order of trial speeds was randomized, and the subjects did not know what the trial speed was going to be. For each trial the subjects were asked to use their preferred manner of locomotion (walking or running). One exception to this was the subject-specific walk-run transition speed, which was tested twice. In the first trial, the subject used their naturally preferred gait; in the second trial, they were instructed to use the other gait (i.e., if the first trial was a walk, then in the second trial they were instructed to run, and vice versa). The subjects were allowed to rest between trials as required.

2.2. Data analysis

The Cartesian coordinate system of the kinematic data collected was such that the *y*-axis was the anteroposterior direction (direction of locomotion), and the *x*-axis was the mediolateral direction. Hence, given that the subject ran in a straight line parallel to the *y*-axis, as constrained by the treadmill, step width was calculated as the difference in the toe marker's *x*-coordinate over successive footfalls. Footfalls were identified based on the vertical (z) coordinate of the toe marker, as well as the vertical component of the ground reaction force data, which was synchronously collected (at 1 kHz). The marker trajectory data was not smoothed or filtered; instead a mean value over the duration of stance was taken in determining the *x*-coordinate for each successive footfall.

3. Bird kinematics

3.1 Data collection

A small indoor racetrack was used for the three quail species, and a larger outdoor one was used for the remaining species. The small racetrack (figure S1a) consisted of an elevated 3 ×

0.4 m wooden trackway, with dark 'hiding places' at either end. The trackway was walled with plywood except part of its lateral side, which was replaced with either clear acrylic (for lateral-anterior camera positions) or fine wire mesh (for anterolateral-posterolateral camera positions). The floor of the trackway was covered with fine grit sandpaper to reduce slippage. A forceplate was also mounted in the middle of the trackway, covered with fine grit sandpaper and flush with the surrounding trackway surface, as part of another study. The large racetrack (figure S1b) consisted of an 11 × 1 m strip of open ground, which was walled on one side by a large shed, and on the other sides by opaque garden plastic. In the middle part of the lateral side of the racetrack, where the birds were filmed, the opaque plastic was replaced by fine wire mesh. Each end of the racetrack had 'hiding boxes' and shade. The top of the racetrack was covered with bird netting, to prevent escape of the birds. A forceplate was also mounted in the middle of the trackway, covered with coarse grit sandpaper and flush with the surrounding trackway surface, as part of another study. It was covered by a plywood board and carpet; the remainder of the racetrack floor was covered by dirt and gravel.

Birds were filmed at a 1280 × 1024 pixel resolution, and at a framerate of usually 250 frames $second^{-1}$. A very small fraction (~6%) of trials were inadvertently filmed at 50–150 frames $second^{-1}$ due to equipment error, but as these trials all pertained to larger bird species which moved at lower stride frequencies, this was of no concern. In the large racetrack setup, the cameras were oriented anterolaterally and posterolaterally relative to the direction of travel, and their orientations relative to one another were separated by at least 60°. A similar set of camera orientations was used for filming the Chinese painted quail in the small racetrack set up, although here the camera separations more closely approached 90°. For the Japanese and northern bobwhite quail, the cameras were oriented anteriorly and laterally to the direction of travel, with the anterior camera placed at one end of the racetrack.

For both racetracks, 3-D wooden frames with markers of known coordinates were used to establish a calibration volume for each day's trials, using an 11-coefficient direct linear transform [6]. The calibration volume for the small racetrack measured approximately 80 × 30 × 20 cm; the calibration volume for the large racetrack measured approximately 140 × 100 × 60 cm. The coordinate system of the calibration volume was such that the x-axis was the direction of travel (anteroposterior direction), the y-axis was left-to-right (mediolateral direction) and the z-axis was vertical.

Prior to data collection, feathers from the back half of the birds were clipped, as were the wings, so as to allow the placement of small (2-5 mm diameter) white markers, and so that the cameras' views of the markers during locomotion was not obstructed. These markers were secured to the skin using double-sided tape. Up to three markers were placed on the midline of the back, along the sacrum, as part of another study. A single marker was placed on the trochanteric crest of both hips, which were easily palpable for all birds studied. Non-toxic, white acrylic paint was used to mark the base of the claw of digit III of both feet.

3.2. Data analysis – present study and ostrich data

Only those trials (or parts thereof) where the bird was moving in a relatively straight line were considered for analysis. Additionally, trials in which the bird displayed obviously abnormal behaviour (e.g., hopping, skipping, alternating pace lengths or sudden lurching to one side) were excluded from analysis; no pathological gaits were observed.

The (x, y) coordinates of the left and right toe markers, as calculated using the DLTdv5 digitizing program [6], were used in the calculation of stride length and step width as follows (figure S2). Firstly, the pace length from one footfall to the next was calculated as

$$D_N = \sqrt{(x_{N+1} - x_N)^2 + (y_{N+1} - y_N)^2}\,, \tag{S7}$$

and stride length at (opposite to) footfall F_N was calculated as

$$S_N = \sqrt{(x_{N-1} - x_{N+1})^2 + (y_{N-1} - y_{N+1})^2}\,. \tag{S8}$$

The enclosed angle φ_N is that angle at footfall F_N which is subtended by the triangle comprising the three consecutive footfalls $\{F_{N-1}, F_N, F_{N+1}\}$, and was calculated as:

$$\varphi_N = \arccos\left(\frac{{D_{N-1}}^2 + {D_N}^2 - S_N}{2D_{N-1}D_N}\right). \tag{S9}$$

If the feet had not crossed over the midline, then this angle was equal to the pace angulation, θ_N. If the feet had crossed over the midline, then the pace angulation in degrees was

$$\theta_N = 360° - \varphi_N. \tag{S10}$$

To determine whether the feet have crossed over the midline required the calculation and comparison of successive 'pace gradients', which are the Cartesian gradients of lines connecting the successive footfalls, as illustrated in figure S2c. Step width at footprint F_N was then calculated in the same manner as for the Culpeper theropod footprints, using equation S3.

The calculations for the bird kinematic data here follow the same convention as outlined above for the Culpeper theropod footprints; if the feet cross over the midline, pace angulation is reflex and step width is negative. To permit fair comparison across birds of differing body size, calculated stride lengths and step widths were then normalized to the standing hip height of the birds using equations S4 and S5.

The data collected for ostriches [7] included 3-D trajectories of a marker on the tip of digit III for both right and left feet. The (x, y) coordinates of the markers during stance phase were extracted and analysed in the same fashion as above. Hip height was determined much in the same way, from a marker placed on the trochanteric crest during trials in which the bird was standing quietly.

3.3. Data analysis – emu data

In the data collected for emus [8], a marker was placed only on the right digit III, in addition to two markers on the midline of the back. As such, the calculations outlined above could not be implemented, and true step width could not be calculated. Step width could nevertheless be estimated, using the trajectory of the back markers as a proxy for the body midline axis (figure S3a). The body midline axis was determined by fitting a least-squares straight line to the (x,y) coordinates of the anterior of the two back markers, since this was the closer of the two to the whole-body COM. Only trials (or parts thereof) in which the bird was moving in a relatively straight line were included in this calculation. This produced the Cartesian equation describing the body axis (figure S3b) as

$$y = mx + c. \tag{S11}$$

Ideally, step width would be twice the distance d from the toe marker coordinates P(x_P,y_P) to the point of its perpendicular intersection with the body axis, I(x_I,y_I). The line IP that connects points I and P has a gradient of

$$m_{IP} = \frac{-1}{m}, \tag{S12}$$

and a y-intercept of

$$c_{IP} = y_P - m_{IP}x_{IP}. \tag{S13}$$

Solving the equations for both lines simultaneously, the coordinates of the intersection point I were calculated as

$$(x_I, y_I) = \left(\frac{c_{IP} - c}{m - m_{IP}}, mx_I + c \right). \tag{S14}$$

In turn, the perpendicular distance was calculated as

$$d = \sqrt{(x_P - x_I)^2 + (y_P - y_I)^2}\ , \tag{S15}$$

and step width estimated as

$$w \approx 2d. \tag{S16}$$

Determining whether the feet have crossed over the (estimated) midline required determining if d was positive or negative. Since the birds always moved from right to left in the experimental setup (towards the ^{-}x direction), if $y_P \geq y_I$, d was positive (no crossover), otherwise it was negative (with crossover). The stride length at (opposite to) a given footfall could not be measured in the manner outlined above for the other species, owing to there being only one toe marker used. Hence, it was estimated by averaging the preceding and following stride lengths, as illustrated in figure S3c. Step width and stride length were then normalized to standing hip height in the same fashion as the other species.

Although the measures of step width and stride length for the emus are different compared to those employed for the other species investigated here, they nevertheless are calculated using the same line of reasoning. It is therefore expected that any relationship between these particular measures will be the same as the relationship between actual step width and stride length, were these available for measurement. It was thus deemed appropriate to maximize the sample of bird data here rather than to exclude the emu data.

4. Statistics

All individuals for a given species were considered together in comparisons of w^* against S^*. To ascertain whether w^* changed in a consistent manner with S^* for a given species, this would normally be tested using linear regression of some form and computing the significance of the slope. As the objective of the current study is to ascertain the overall relationship between w^* and S^*, rather than to predict one from the other, the most appropriate method of line fitting is major axis (MA) regression [9]. The data was found to fail two assumptions of standard parametric tests of the slope, however, as determined in PAST 3.09 [10]; namely, non-normal distribution of errors and heteroscedasticity (using the Breusch-Pagan test). Consequently, a permutation test was used instead [11], implemented in a custom MATLAB script. For each species, the MA slope was determined; the values of w^* were then randomly rearranged with respect to S^* and the MA slope recomputed. A total of 100,000 replicates were conducted for each species' data set. The significance (P-value) of

the MA slope is the proportion of replicates for which the calculated MA slope is equal to or more extreme than the actual MA slope of the data.

After identifying those datasets that showed w^* to decrease significantly with S^*, three types of curve were fit to each using least squares: linear, power and logistic. The Akaike Information Criterion was then used to ascertain which type of curve was the best model of a given dataset, as calculated in R 3.2.2 (R Foundation, Vienna, Austria); the results of this undertaking are reported in table S1. This helped identify whether there was a discontinuity in the data (best fit by a logistic function) or not (best fit by a linear or power function). In identifying whether a given dataset was better fit by a continuous or discontinuous function, this approach was not an attempt to more accurately model the data, and as such the results should not be used for predictive or explanatory purposes. In already knowing that w^* decreases with S^* (via the MA test above), the purpose of this approach was simply to help elucidate *how* the decrease occurred.

5. Visualizing patterns in the data

For both the theropod footprint and bird kinematic data, there was often a considerable amount of scatter and bias in the plot of w^* versus S^*. In the case of the theropod footprints, this was concentrated toward lower values of S^*, stemming from a large proportion of the footprints being made at slower walking speeds ($S^* \approx 1.5–1.7$). One possible explanation for the large scatter in w^* at lower values of S^* is that a slow walking theropod (avian or non-avian) may exhibit greater variation in step width as a result of 'wandering', perhaps because they are looking for food or assessing their surroundings. Additionally, at faster speeds of locomotion, the body has greater forward-directed linear momentum (as discussed in the main text), increasing the propensity for it to move in a straighter line with less 'wander'.

To reduce the above scatter and bias, the individual values of w^* were binned into set, equal intervals of S^*, and means were subsequently taken for each bin, permitting a comparison of narrow intervals of S^* versus the mean w^* for each interval (figures 2b, 4). As the sample size for each species was varied, two different bin interval sizes were used. In those species for which $n \geq 200$ (including the theropod footprint data), an interval of 0.05 was used; in those species for which $n < 200$, a coarser interval of 0.1 was used, so as to have sufficient data points within most bins for the averages to be meaningful. This approach was used purely as a visualization tool, to help improve the detection and appreciation of underlying patterns in the

raw data; it was the raw data itself that was used in all quantitative analyses undertaken. The validity of binning approach was demonstrated by the fact that MA regression lines, calculated from the raw data, neatly fitted the scatterplot of the binned data as well. Furthermore, the result of binning does not change when the bin intervals are altered. For instance, doubling the bin interval width of the Culpeper theropod footprint data did not change the overall pattern, nor did shifting the interval span along the S^* axis by half of the interval width.

Supplementary figures

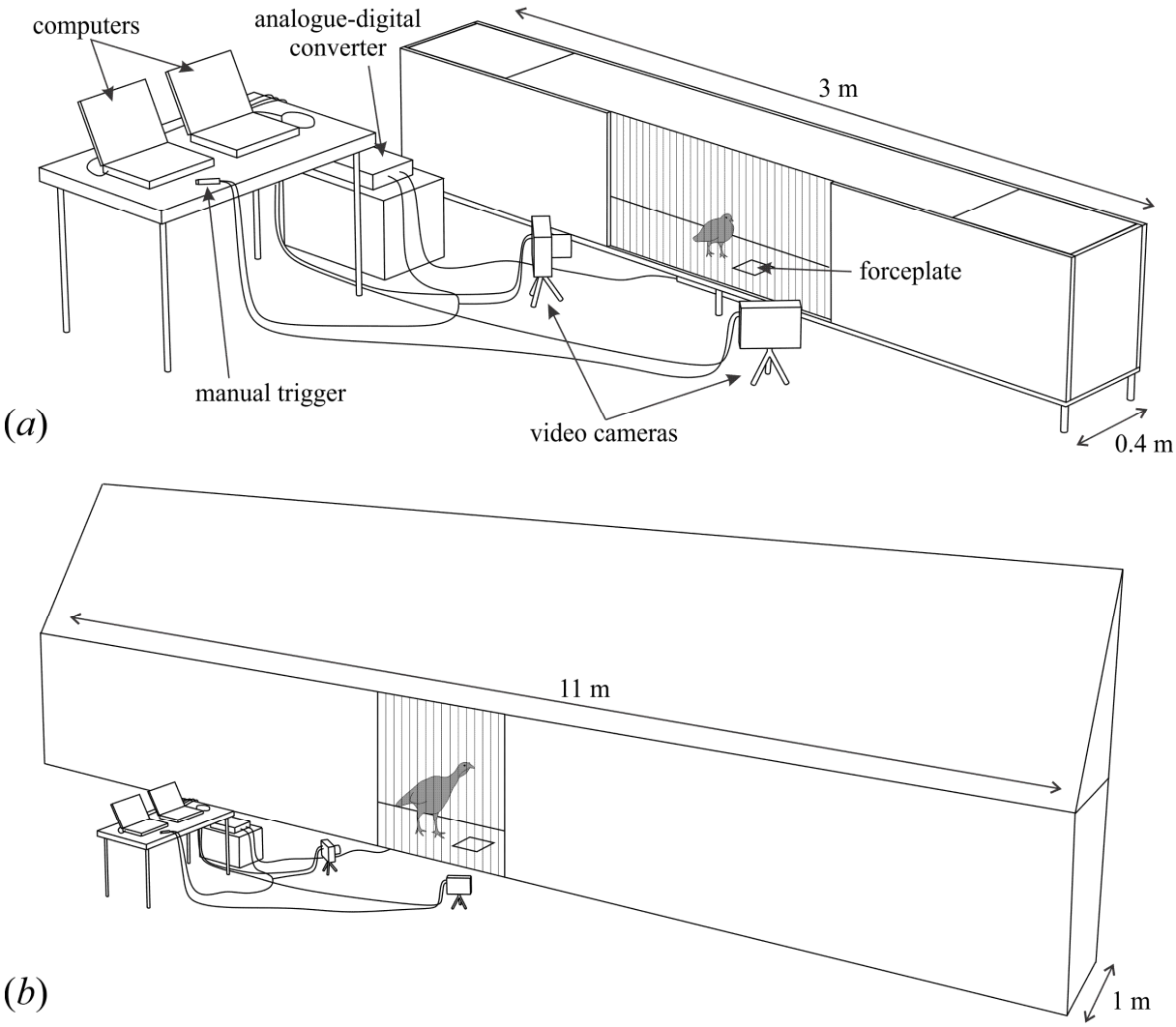

Figure S1. Diagrammatic illustration of the experimental setups used to obtain bird kinematics. (*a*) Small racetrack used for the three quail species. (*b*) Large racetrack used for the remaining species. Forceplates were also present in both racetracks as part of another study; these were mounted flush with the surrounding track surface and were covered with fine grit sandpaper.

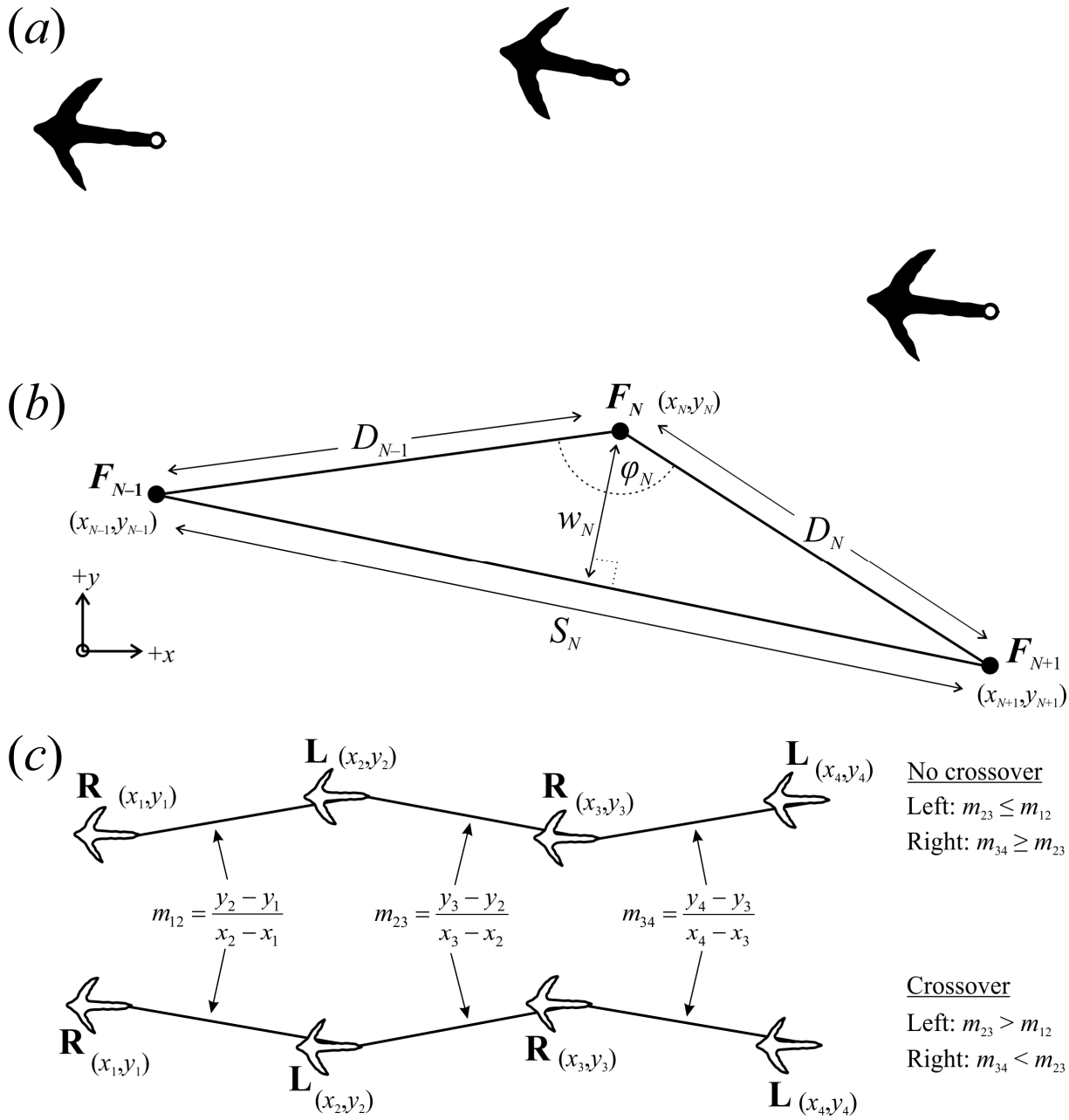

Figure S2. The calculation of step width and stride length in birds. (*a*) The common point of reference for measurements was the base of the claw of digit III. (*b*) From the (*x*,*y*) coordinates of the toe markers, the pace length *D* , stride length *S*, enclosed angle φ and step width *w* were calculated (see text for formulae). (*c*) Whether step width was positive or negative depends on whether crossover of the right (R) and left (L) feet had occurred or not. This can be determined by comparing the Cartesian gradients of lines connecting successive footfalls. These patterns hold true regardless of whether the bird is moving from left to right (i.e., *x* values are increasing) or right to left (i.e., *x* values are decreasing).

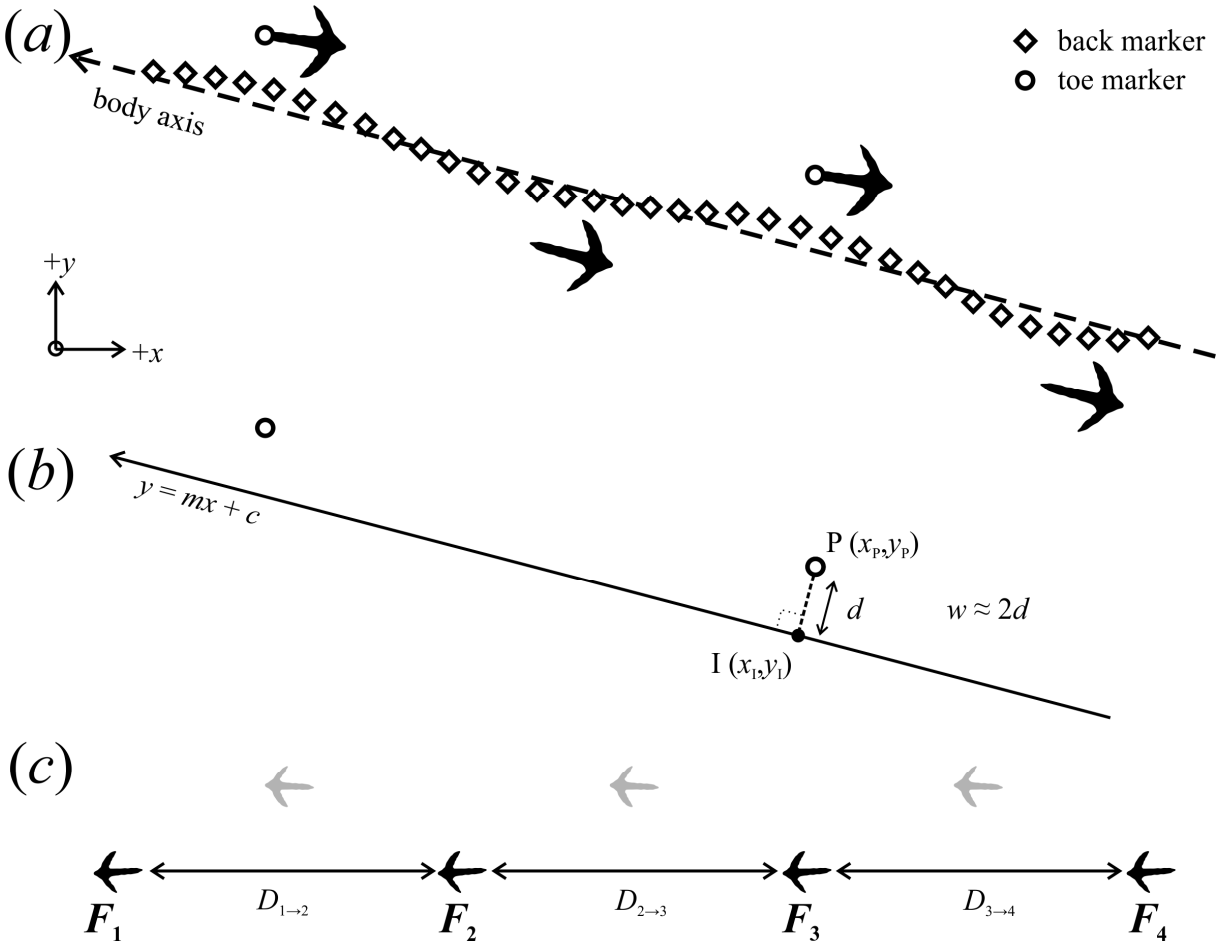

stride length at footfall F_n, in a sequence of N footfalls:

$$S_1 = D_{1\to 2}$$

$$S_n = \frac{D_{n-1\to n} + D_{n\to n+1}}{2}$$

$$S_N = D_{N-1\to N}$$

Figure S3. The calculation of step width and stride length in emus, using the data collected previously [8]. (*a*) The common point of reference for measurement was the end of digit III on the right foot during stance. In addition, the trajectory of a back marker was used to define a 'body axis', by fitting a straight line through the marker trajectory. (*b*) From the (*x*,*y*) coordinates of the toe marker and the Cartesian equation of the body axis, the perpendicular distance *d* can be calculated, and in turn step width estimated. (*c*) Stride length at a particular footfall was estimated by averaging the preceding and following stride lengths, except for the first and last footfall, for which the first and last stride length were used, respectively.

Supplementary table

Table S1. Results of curve-fitting analysis used to assess whether *w** changed with *S** in a continuous (major axis linear or power model) or discontinuous (logistic model) fashion. Akaike Information Criterion (AIC) values that are the lowest for each dataset, indicating the best fit, are in bold. Only datasets that showed *w** to decrease significantly with *S** (demonstrated by the MA tests) were subject to the curve fitting analysis. For this reason, and because of non-normality or heteroscedasticity in many of the datasets, computing statistical significance of these fits is not useful.

	Linear coefficients		**Power coefficients**		**Logistic coefficients**			**AIC**		
Dataset	***a***	***b***	***a***	***b***	***a***	***b***	***c***	**linear**	**power**	**logistic**
Non-avian theropod footprints	-0.0396	0.1080	0.2197	-3.4269	152.0547	-2.4845	-1.67151	-1985	**-2042**	-2039
Humans	-0.1327	0.3193	0.2295	-2.1092	0.13956	-8.0492	1.90142	-1401	-1382	**-1561**
T. moluccus	-0.1067	0.4388	0.8820	-1.8315	77.3501	-0.7296	-5.90865	**-277.6**	-262.3	-259.1
M. gallopavo	-0.0081	0.0814	0.0845	-0.4136	12.6832	-0.1598	-30.9897	-424.5	**-487.5**	-484.8
D. novaehollandiae	-0.0268	0.0654	0.0549	-2.1024	0.0262	-9.2911	1.918594	**-4670.5**	-3873	-3882
S. camelus	-0.0411	0.0788	64.5626	-43.3112	19.4411	-36.1769	1.015416	-104.6	**-108.6**	-106.6
P. porphyrio	-0.0209	0.0991	0.4509	-2.4476	0.0451	-4.5517	3.931852	30.6	**-95.1**	-94.5

Linear model has the form $f(x) = ax + b$; power model has the form $f(x) = ax^b$; logistic model has the form $f(x) = \frac{a}{1+e^{-b(x-c)}}$, where *e* is the base of natural logarithms.

Supplementary references

[1] Weems, R.E. 1992 A re-evaluation of the taxonomy of the Newark Supergroup saurischian dinosaur tracks, using extensive statistical data from a recently exposed tracksite near Culpeper, Virginia. *Virginia Division of Mineral Resources Publication* **119**, 113-127.

[2] Weems, R.E. 2006 Locomotor speeds and patterns of running behaviour in non-maniraptoriform theropod dinosaurs. *New Mexico Museum of Natural History and Science Bulletin* **37**, 379-389.

[3] Thulborn, R.A. 1984 Preferred gaits of bipedal dinosaurs. *Alcheringa* **8**, 243-252.

[4] Thulborn, R.A. & Wade, M. 1984 Dinosaur trackways in the Winton Formation (mid-Cretaceous) of Queensland. *Memoirs of the Queensland Museum* **21**, 413-517.

[5] Thulborn, T. 1990 *Dinosaur Tracks*. London, Chapman and Hall.

[6] Hedrick, T.L. 2008 Software techniques for two- and three-dimensional kinematic measurements of biological and biomimetic systems. *Bioinspiration & Biomimetics* **3**, 034001.

[7] Rubenson, J., Lloyd, D.G., Besier, T.F., Heliams, D.B. & Fournier, P.A. 2007 Running in ostriches (*Stuthio camelus*): three-dimensional joint axes alignment and joint kinematics. *Journal of Experimental Biology* **210**, 2548-2562.

[8] Lamas, L.P. 2015 Musculoskeletal biomechanics during growth on emu (*Dromaius*; Aves): An integrative experimental and modelling analysis. [PhD], Royal Veterinary College, University of London.

[9] Warton, D.I., Wright, I.J., Falster, D.S. & Westoby, M. 2006 Bivariate line-fitting methods for allometry. *Biological Reviews* **81**, 259-291.

[10] Hammer, Ø., Harper, D.A.T. & and Ryan, P.D. 2001 PAST: Paleontological Statistics Software Package for Education and Data Analysis. *Palaeontologia Electronica* **4**, 4.

[11] Legendre, P. & Legendre, L. 2012 *Numerical Ecology, Third English Edition*. Amsterdam, Elsevier.